

# FREQUENCY STABILITY OF GPS NAVSTAR BLOCK I AND BLOCK II ON-ORBIT CLOCKS

Thomas B. McCaskill  
Wilson G. Reid  
James A. Buisson  
U.S. Naval Research Laboratory  
Washington, D.C., 20375

and  
Hugh E. Warren  
Sachs Freeman Associates, Inc.

## *Abstract*

*Analysis of the frequency stability of on-orbit NAVSTAR clocks is performed by the Naval Research Laboratory. This work was sponsored by the GPS Joint Program Office. The frequency stability is presented for sample times of one day to 30 days. Composite frequency-stability profiles are presented for the Block I and Block II NAVSTAR clocks. Several NAVSTAR cesium clocks show frequency stabilities of a few parts in  $10^{14}$  for long sample times. Time-domain noise-process analysis shows the dominant noise type to be white frequency noise for sample times of one to ten days. The non-stationary stochastic behavior of one of the cesium clocks, illustrated by its frequency-stability history, shows that the frequency stability is not always time-invariant.*

## INTRODUCTION

The Naval Research Laboratory determines on-orbit NAVSTAR clock performance using the process depicted in Figure 1. The analysis includes frequency and aging histories, frequency-stability profiles, time-prediction uncertainty profiles, time-domain noise process profiles, spectral analysis, and anomaly detection. Events that perturb the normal clock performance are of particular interest.

The results of the on-orbit analysis represent the behavior of the NAVSTAR clock with system errors superimposed. The influence of the system may enhance but usually degrades the observed performance of the clock. Therefore, deviations from nominal performance are analyzed in an attempt to identify the cause.

The Block I data was collected by the U.S. Naval Observatory using a single-frequency, time-transfer receiver with ionospheric corrections obtained from the model of the ionosphere broadcast in the navigation message. The Block II data was collected using a dual-frequency, authorized-user, time-transfer receiver which measures the ionospheric delay and automatically corrects for selected

availability (S/A). In both cases, the broadcast ephemeris is used by the receiver in computing the theoretical range from the monitor site to the space vehicle at the time of measurement. Table 1 summarizes the data used in the analysis.

*Table 1*  
**DATABASE**  
**GPS BLOCK I AND BLOCK II CLOCKS**  
U.S. Naval Observatory Monitor Site

NAVSTAR Number	SV Number	Block Number	Clock Serial	Clock Type	Time Span mjd      mjd days
3	6	I-3	20	Rb	8439-8571      133
8	11	I-8	2	Cs	6569-8571      2003
9	13	I-9	4	Cs	5894-8571      2678
10	12	I-10	5	Cs	5984-8571      2588
11	3	I-11	12	Rb	6369-8571      2203
14	14	II-1	8	Cs	7705-8571      867
13	2	II-2	14	Cs	7719-8571      853
16	16	II-3	11	Cs	8266-8571      306
19	19	II-4	27	Cs	7852-8571      720
17	17	II-5	25	Cs	7900-8571      672
18	18	II-6	31	Cs	7936-8571      636
20	20	II-7	30	Cs	8009-8571      562
21	21	II-8	6	Cs	8126-8400      275
15	15	II-9	37	Cs	8180-8571      392
23	23	II-10	36	Cs	8263-8571      309
24	24	II-11	52	Cs	8482-8571      90

The Block I space vehicles included in this analysis were not equipped with selective availability. Therefore, the data collected from these space vehicles by the single-frequency receiver was unaffected when S/A was implemented.

The clock offset is measured using a sequence of pseudorange measurements and the predicted range obtained from the space-vehicle orbital elements broadcast in the navigation message. The clock offset measurements are then smoothed over each non-overlapping 13-minute interval. The measurement representing a pass is the 13-minute measurement nearest the time of closest approach, or the one having the highest elevation angle, which minimizes the effect of the ionosphere on the measurement.

Time and frequency inputs to the time-transfer receiver were derived from the Observatory master clock which is a physical realization of the time scale generated by the Observatory from an ensemble of several types of atomic frequency standards. Since the stability of the time-scale is significantly better than that of an individual NAVSTAR clock, the measurements made by the Observatory reflect primarily the behavior of the NAVSTAR clocks.

The frequency stability of the Block I NAVSTAR clocks was computed using sample times from one day to a maximum of 30 days. In all cases the length of the database is a factor of ten, or more, greater than the maximum sample time evaluated. A long-term aging correction was determined

for each NAVSTAR clock and was removed from the data before computing the frequency stability.

## BLOCK I NAVSTAR CLOCK PERFORMANCE

Figure 2 presents the frequency offset as a function of time for the NAVSTAR 3 rubidium clock. This is the second NAVSTAR 3 rubidium clock to be activated—the first having been activated in 1978 and having operated successfully for 13 years. The eclipse seasons are depicted by the shaded regions that repeat at a nominal rate of once every six months. The data shows large frequency fluctuations that appear to be related to the eclipse season. Previous analysis by the Naval Research Laboratory determined that the frequency offset of the first rubidium clock was sensitive to temperature and exhibited a temperature coefficient of  $1.96 \times 10^{-12}/^{\circ}\text{C}$ . It is expected that the current rubidium clock will exhibit a similar temperature coefficient. It should be noted that beginning with NAVSTAR 8 all rubidium clocks had additional thermal control which appears to have isolated the clock from seasonal temperature variations.

Figure 3 presents the frequency offset for the NAVSTAR 8 cesium clock for a period of almost six years while Figures 4 and 5 present the frequency offset for the NAVSTAR 9 and NAVSTAR 10 cesium clocks for a period of more than seven years. The frequency offset for the clock on NAVSTAR 10 shows two knees in the data where the aging abruptly increased.

Figure 6 presents the frequency offset for the NAVSTAR 11 rubidium clock for a period of three years. The vertical scale has been expanded by plotting the residuals to a linear fit of the data. The sensitivity to temperature is evident in the wide seasonal swings in the frequency offset—similar to those seen previously on the first NAVSTAR 3 rubidium clock—with a fundamental period of nominally one year, although eclipse seasons occur every six months. Unlike that clock, however, the NAVSTAR 11 rubidium clock exhibits a negative temperature coefficient.

A composite of the frequency-stability profiles for all Block I NAVSTAR clocks operating on 11 November 1991 is presented in Figure 7. Of the five NAVSTAR clocks currently operating, two are rubidium and three are cesium. During 1991 all but NAVSTAR 10 had frequency stabilities less than  $2 \times 10^{-13}$  for a one-day sample time. The other two cesium clocks demonstrated excellent performance for all sample times that were evaluated. The stability varied from  $1.8 \times 10^{-13}$  at one day to  $3.8 \times 10^{-14}$  at 30 days. The NAVSTAR 10 cesium clock is well past its design life of five years during which time it performed within the specification of  $2.0 \times 10^{-13}$ . This can be seen from the frequency-stability history in Figure 8 which corresponds to the output of a 20-day moving average filter operating on the sequence of squared first differences of the one-day frequency offset measurements shown in Figure 5. The frequency stability of the two NAVSTAR rubidium clocks for an increasing sample time suffers from the wide swings in the frequency due to the seasonal temperature variations.

## BLOCK II NAVSTAR CLOCK PERFORMANCE

Figure 9 presents the corrected frequency offset for the NAVSTAR 14 cesium clock over a two-year time span. The corrected frequency offset had a measured aging coefficient of  $-3.2 \times 10^{-16}/\text{day}$  during the two-year span. Note a small change in the behavior of the frequency offset beginning near mjd 8150 (16 September 1990). After this date the frequency offset showed a change from white noise (uncorrelated) to slow fluctuations in the data. The presence of these fluctuations in

the data degrade the stability at larger sample times as will be seen from the frequency-stability profile.

Figure 10 presents the corrected frequency offset for the NAVSTAR 13 cesium clock. The frequency offset is well behaved with an aging coefficient of  $-1.79 \times 10^{-15}/\text{day}$ .

Figure 11 presents the corrected frequency offset for the NAVSTAR 16 cesium clock. The frequency offset shows slow fluctuations in the data that persist throughout 1991. The average aging during this eleven-month time span was  $-2.61 \times 10^{-15}/\text{day}$ . The phase offset for the first portion of the data was compared to that obtained using the precise ephemeris computed by the Defense Mapping Agency. The precise ephemeris yielded the same behavior which indicates that the accuracy of the broadcast ephemeris is not responsible for the observed behavior which is not characteristic of ground-based cesium clocks and has not been observed in the Block I cesium clocks.

Figure 12 presents the frequency offset for the NAVSTAR 19 cesium clock from shortly after initial turn-on to 11 November 1991. Anomalies in the form of sharp decreases in the frequency offset by as much as  $-7 \text{ pp}10^{13}$  repeated at intervals of between 35 to 54 days began about 9 May 1989. Prior to occurrence of the first anomaly and during the subsequent intervals between the periodic breaks the clock exhibited an aging of about  $1.63 \text{ pp}10^{14}/\text{day}$  which is rather high for a cesium clock. The aging exhibited during the initial period after turn-on and during the first twelve cycles appears to have changed appreciably at the beginning of the last cycle to approximately  $5.0 \text{ pp}10^{14}/\text{day}$ . The frequency stability was computed for the first 200 days and for the entire time span. The stability for the first segment is included in a composite stability plot. The stability for the entire time span marginally meets the Block II specification of  $2 \times 10^{-13}$  for sample times of one to ten days.

Figure 13 presents the corrected frequency offset for the NAVSTAR 17 cesium clock. The frequency offset from mjd 7900 to mjd 8068 was well behaved. An abrupt decrease in frequency on mjd 8068 was followed by a partial recovery. Then again on mjd 8195 the frequency appears to have further recovered. A comparison of the frequency stability for the period prior to mjd 8068 and again for the period after mjd 8195 showed a small degradation in the frequency stability for a one-day sample time following the frequency anomaly. The aging that occurred in the data during 1991 was  $-1.40 \times 10^{-15}/\text{day}$ .

Figure 14 presents the corrected frequency offset for the NAVSTAR 18 cesium clock. The frequency offset shows a small positive excursion beginning at mjd 8195—that correlates with the same behavior on the NAVSTAR 17 cesium clock. The data subsequent to this time appears to be noticeably quieter. The aging during 1991 for the NAVSTAR 18 cesium clock was  $-5.00 \times 10^{-17}/\text{day}$ .

Figure 15 presents the corrected frequency offset for the NAVSTAR 20 cesium clock. The frequency offset exhibits a small positive aging from initial operation and appears to have a small negative rate of change of aging. Except for the small apparent change in aging the data appears to be well behaved. The average aging during 1991 was  $1.39 \times 10^{-15}/\text{day}$ .

Figure 16 presents the corrected frequency offset for the NAVSTAR 21 cesium clock. Two frequency shifts, followed by recovery to the nominal frequency offset occurred on mjd 8451 and on mjd 8504. The cause of these unexpected shifts in the frequency is being investigated. The average aging before the shifts was  $-1.74 \times 10^{-15}/\text{day}$ . The frequency stability presented later in the composite plot of frequency stability was computed for the data before the shifts in frequency.

Figure 17 presents the corrected frequency offset for the NAVSTAR 15 cesium clock. The frequency appears well behaved and exhibited an aging during 1991 of  $-2.8 \times 10^{-16}/\text{day}$ .

Figure 18 presents the corrected frequency offset for the NAVSTAR 23 cesium clock. The frequency offset is well behaved and exhibited an aging during 1991 of  $2.7 \times 10^{-16}/\text{day}$ . Noteworthy is the fact that this is the first of the Block II-A NAVSTAR space vehicles.

Figure 19 presents the frequency offset for the NAVSTAR 24 cesium clock. The cause of the anomalous behavior occurring before 30 August 1991 (mjd 8498) may be attributed to a period of testing of the space vehicle. Only the data in the span of time from 30 August 1991 (mjd 8498) to 11 November 1991 was used in the calculation of the frequency stability. The aging following mjd 8498 was  $2.06 \times 10^{-15}/\text{day}$ .

A composite of the frequency-stability profiles for all Block II NAVSTAR clocks operating on 11 November 1991 is presented in Figure 20. An individual long-term aging correction was calculated for each NAVSTAR clock and removed before computing the frequency stability. The Block II frequency-stability profiles show that all of the NAVSTAR cesium clocks were within the  $2 \times 10^{-13}$  specification for a one-day sample time and had stabilities of less than the specification for all sample times up to 30-days. The dominant random noise types observed for the cesium clocks was white frequency noise for sample times of one to ten days with a gradual trend towards flicker frequency noise for sample times of 30-days. This was the expected frequency profile for well behaved cesium clocks. Small departures from white frequency noise towards random walk frequency noise were noted for several of the cesium clocks. This is believed to be due to small anomalies in the frequency offset rather than to the presence of any significant component of random walk in the frequency.

## CONCLUSIONS

The frequency stability for four of the five Block I NAVSTAR clocks was better than the specification of  $2 \times 10^{-13}$  for Block I cesium clocks for a sample time of one-day. The NAVSTAR-10 cesium clock, which has exceeded the design life, did not meet the one-day frequency-stability specification during 1991.

All Block II NAVSTAR cesium clocks are better than the  $2 \times 10^{-13}$  specification for a one-day sample time. The best frequency stability for a one-day sample time was  $8 \times 10^{-14}$ . The dominant random noise type for the Block II NAVSTAR cesium clocks was white frequency noise for sample times of one to ten days.

The performance for all Block I and Block II clocks operating on 11 November 1991 is summarized in Table 2.

Table 2

PERFORMANCE SUMMARY  
 GPS BLOCK I AND BLOCK II CLOCKS  
 U.S. Naval Observatory Monitor Site  
 Calendar 1991

Navstar Number	Clock Serial	Clock Type	Time Span (days)	Frequency			Aging 1991 (pp10 <sup>15</sup> /day)
				Stability 1 day (pp10 <sup>13</sup> )	10 days (pp10 <sup>14</sup> )		
3	20	Rb	132	1.8	41.4	28.50	
8	2	Cs	314	1.8	4.9	0.37	
9	4	Cs	314	1.8	5.4	-0.57	
10	5	Cs	314	3.6	9.3	-12.80	
11	23	Rb	314	1.5	23.6	-124.00	
14	8	Cs	314	1.2	5.2	-0.32	
13	14	Cs	314	1.5	4.3	-1.79	
16	11	Cs	305	1.4	7.4	-2.61	
19	27	Cs	208	1.7	9.6	16.30	
17	25	Cs	314	1.1	4.3	-1.40	
18	31	Cs	314	1.0	3.7	0.05	
20	30	Cs	314	1.3	3.8	1.39	
21	6	Cs	327	1.4	5.7	-1.74	
15	37	Cs	314	1.7	5.6	-0.28	
23	36	Cs	308	1.1	3.3	0.27	
24	52	Cs	73	0.8		2.06	

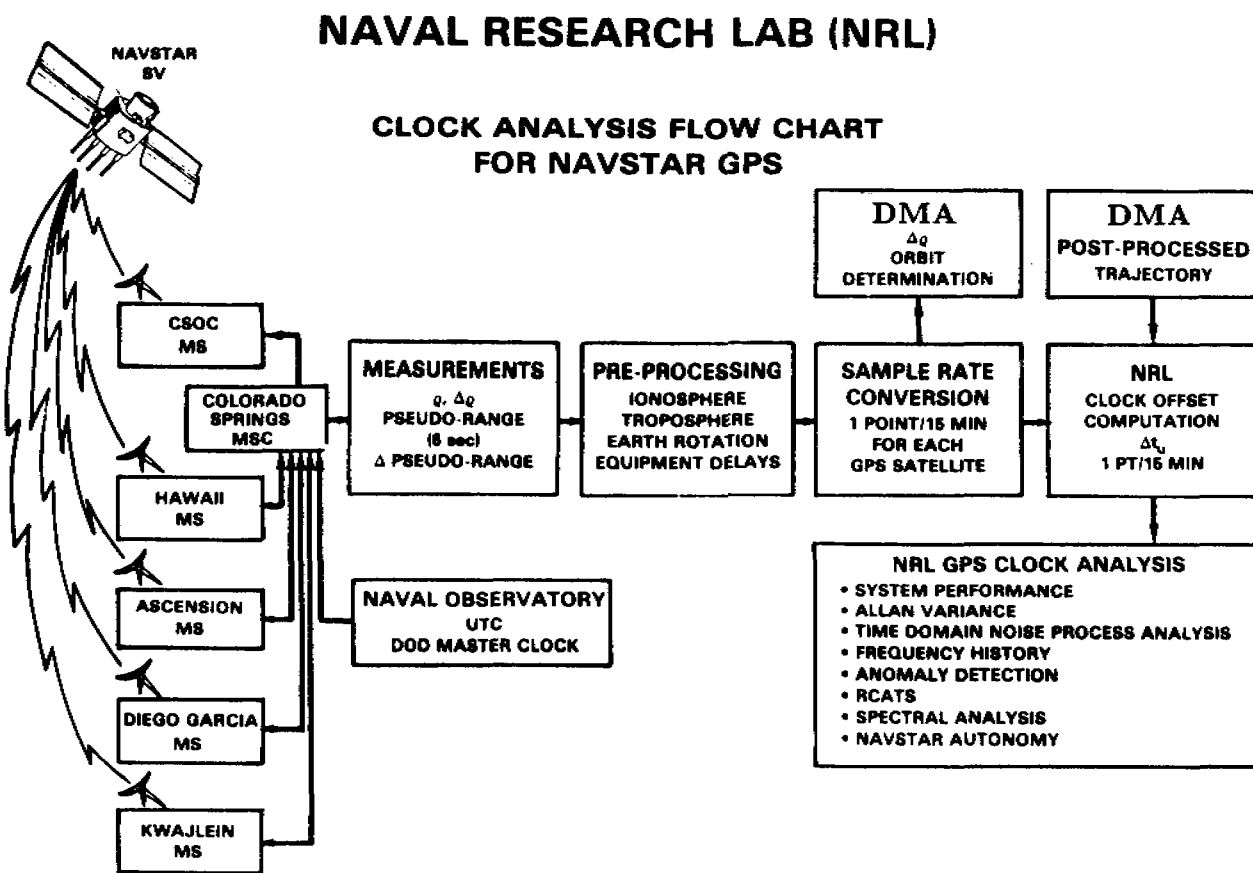


Figure 1. Clock Analysis Flow Chart.

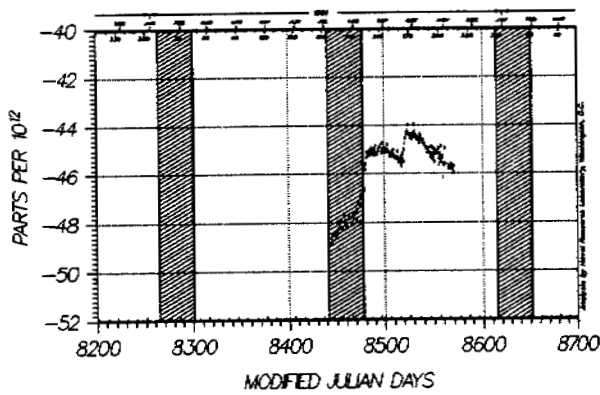


Figure 2. NAVSTAR 3 Frequency Offset.

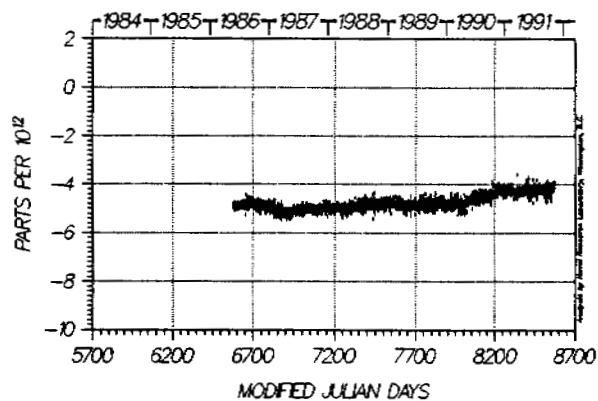


Figure 3. NAVSTAR 8 Frequency Offset.

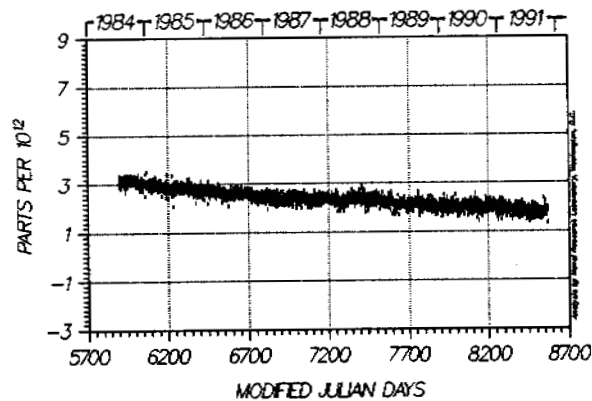


Figure 4. NAVSTAR 9 Frequency Offset.

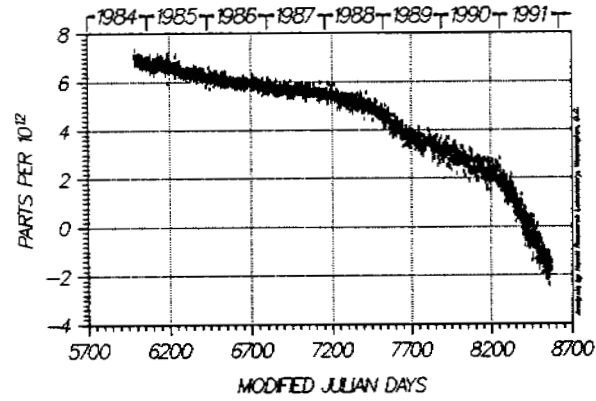


Figure 5. NAVSTAR 10 Frequency Offset.

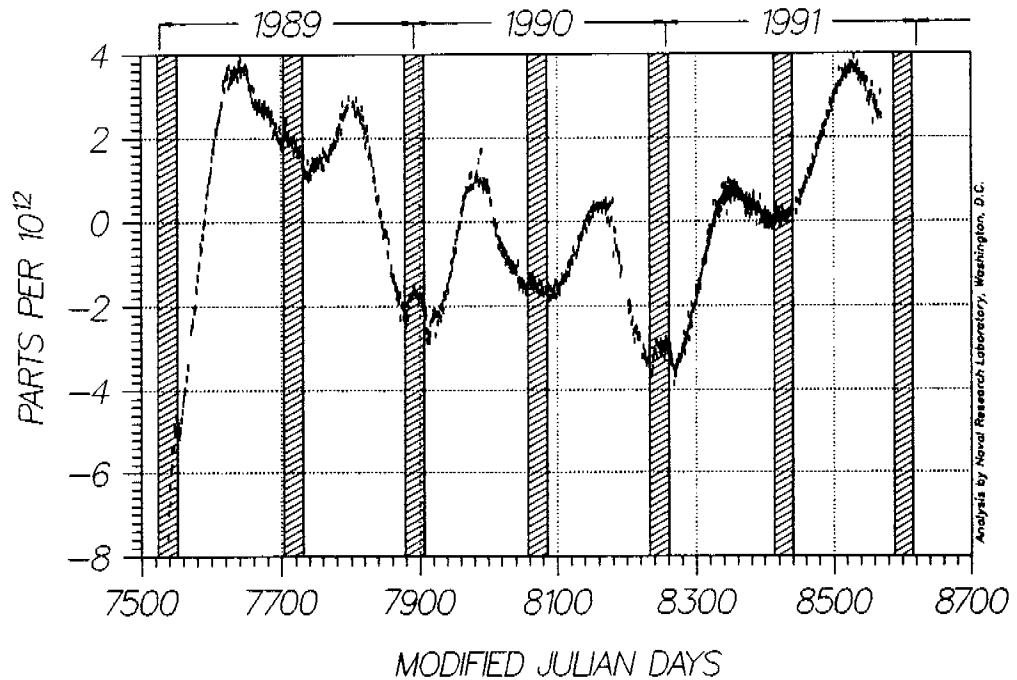


Figure 6. NAVSTAR 11 Frequency Offset.

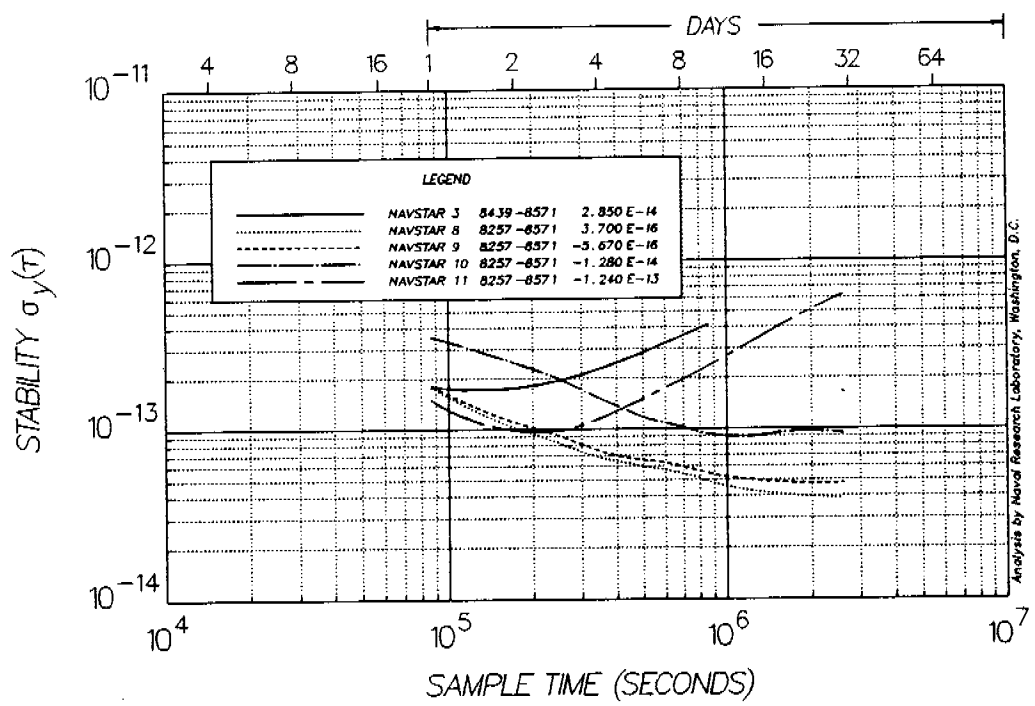


Figure 7. Block I Composite Stability.

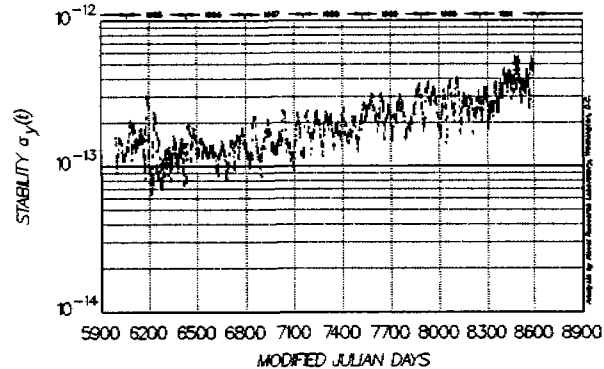


Figure 8. NAVSTAR 10 Stability History.

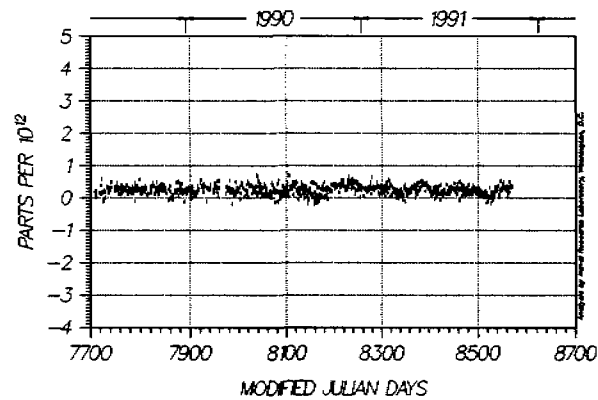


Figure 9. NAVSTAR 14 Frequency Offset.

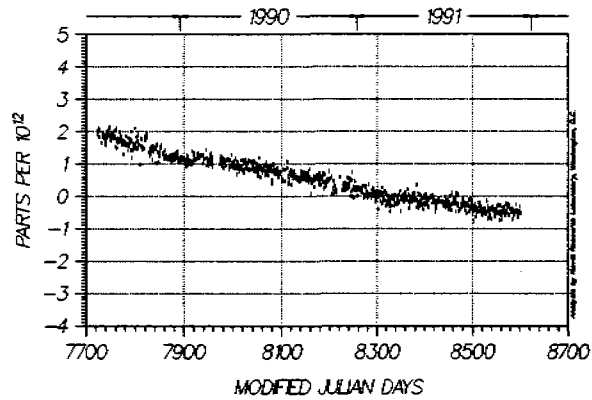


Figure 10. NAVSTAR 13 Frequency Offset.

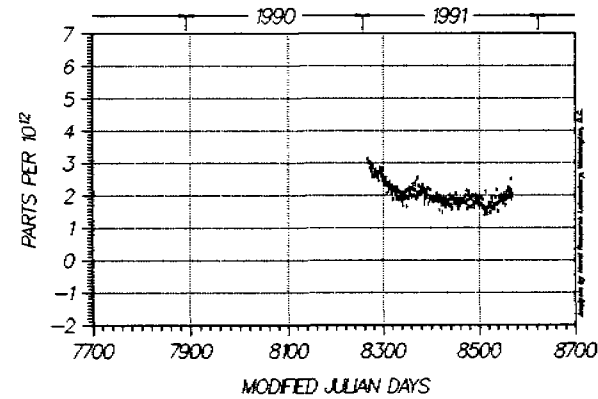


Figure 11. NAVSTAR 16 Frequency Offset.

L1C

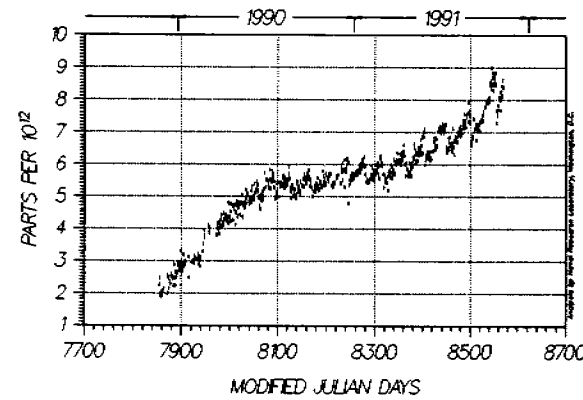


Figure 12. NAVSTAR 19 Frequency Offset.

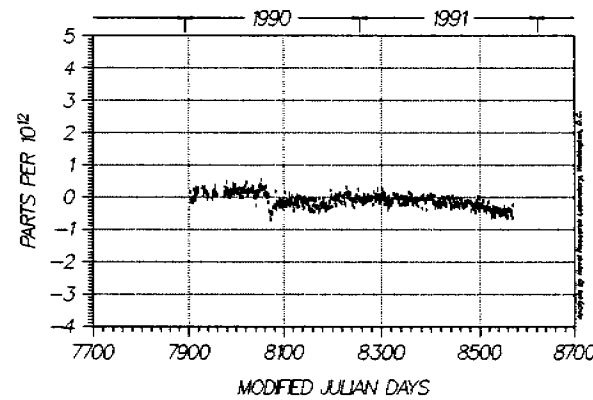


Figure 13. NAVSTAR 17 Frequency Offset.

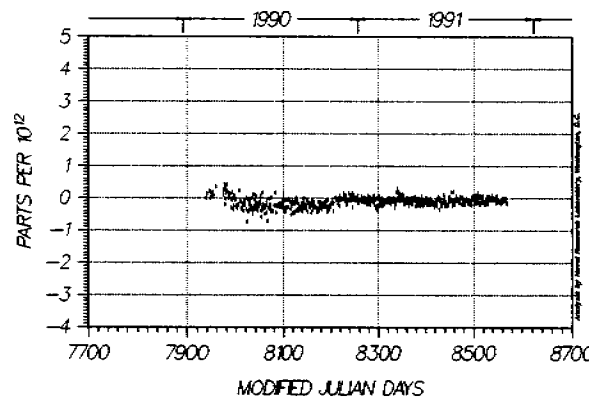


Figure 14. NAVSTAR 18 Frequency Offset.

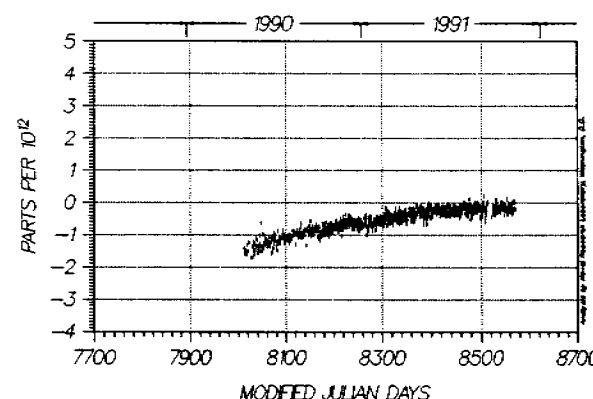


Figure 15. NAVSTAR 20 Frequency Offset.

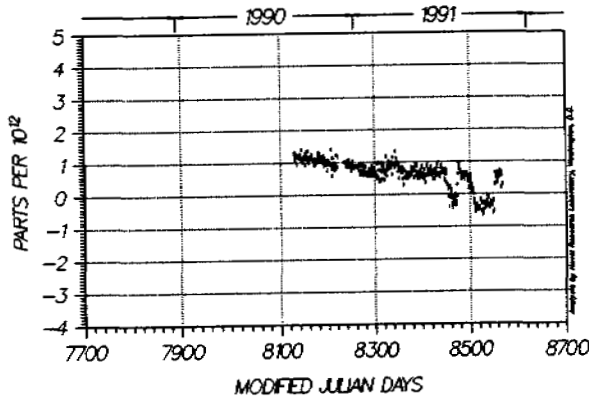


Figure 16. NAVSTAR 21 Frequency Offset.

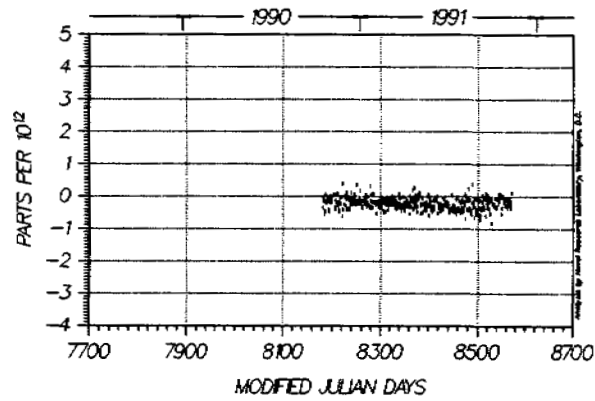


Figure 17. NAVSTAR 15 Frequency Offset.

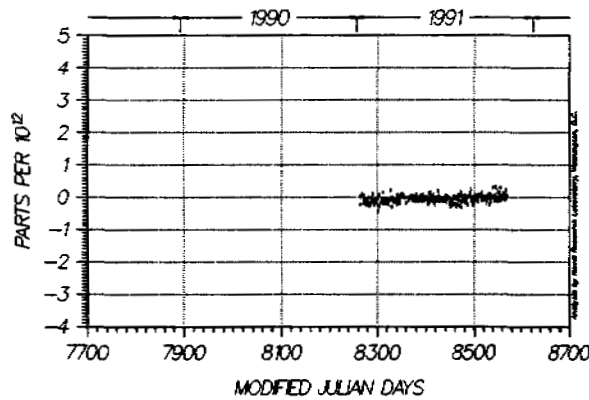


Figure 18. NAVSTAR 23 Frequency Offset.

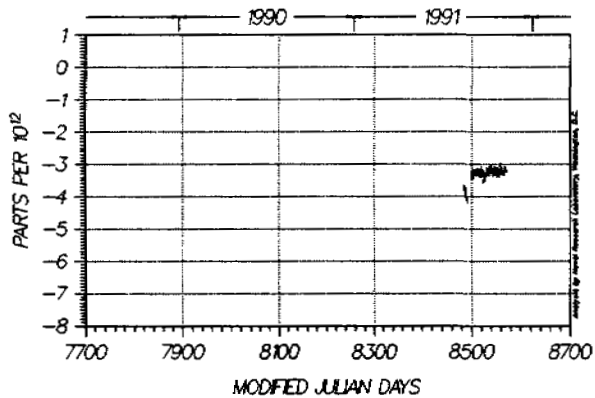


Figure 19. NAVSTAR 24 Frequency Offset.

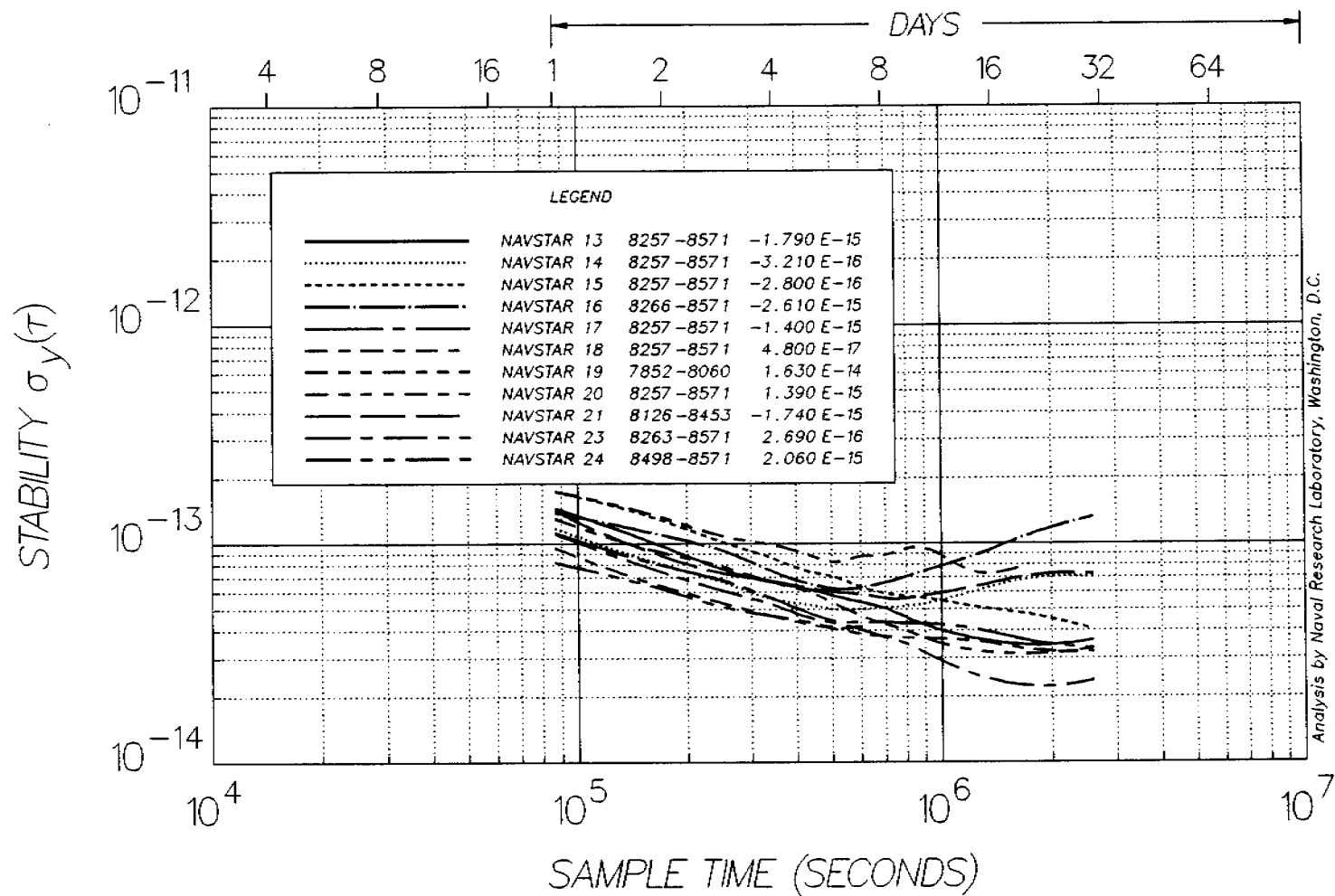


Figure 20. Block II Composite Stability.